



Article

Remote Sensing Based Spatial-Temporal Monitoring of the Changes in Coastline Mangrove Forests in China over the Last 40 Years

Junyao Zhang ^{1,2}, Xiaomei Yang ^{1,2}, Zhihua Wang ^{1,2}, Tao Zhang ^{3,*} and Xiaoliang Liu ¹

- ¹ State Key Laboratory of Resources and Environmental Information System, Institute of Geographic Sciences and Natural Resources Research, Chinese Academy of Sciences, Beijing 100101, China; zhangjy@reis.ac.cn (J.Z.); yangxm@reis.ac.cn (X.Y.); zhwang@reis.ac.cn (Z.W.); liuxiaoliang@reis.ac.cn (X.L.)
- ² University of Chinese Academy of Sciences, Beijing 100049, China
- ³ Land Satellite Remote Sensing Application Center (LASAC), Beijing 100048, China
- * Correspondence: zhangt@reis.ac.cn

Abstract: As a developing country, China's mangrove landscape pattern has undergone significant temporal and spatial changes over the last four decades. However, we know little about the changes in the mangrove landscape pattern characteristics other than the area at the national scale. The analysis of mangrove landscape pattern changes from different perspectives on a national scale can provide scientific support for mangrove protection and restoration. In this study, the temporal and spatial changes in the pattern of the mangrove landscape over the last 40 years in China were analyzed based on remote sensing data with high classification accuracy (99.3% of 2018). First, according to the natural geographical conditions of the coastal zone and the distribution of the mangroves, the distribution area of the mangroves in China was divided into 31 natural shores. Then, by selecting representative landscape indexes and constructing an integrated landscape index, the spatial-temporal changes in the landscape pattern of China's mangroves over the last 40 years were analyzed based on five perspectives: Total area change, shape complexity, connectivity, fragmentation, and the integrated state of the landscape. From a temporal viewpoint, before 2000, the total area of each shore exhibited a downward trend, and the degree of connectivity deteriorated continuously, but the degree of fragmentation was stable at a low level. After 2000, although the total area improved, the degree of fragmentation gradually increased. The spatial changes are mainly reflected by the fact that the shores in Guangdong and Hainan exhibited significant differences within the same province. Based on the above analysis, corresponding scientific suggestions are proposed from temporal and spatial viewpoints to provide guidance for mangrove management and protection in China and to provide a reference for mangrove research in other regions of the world.



Citation: Zhang, J.; Yang, X.; Wang, Z.; Zhang, T.; Liu, X. Remote Sensing Based Spatial-Temporal Monitoring of the Changes in Coastline Mangrove Forests in China over the Last 40 Years. *Remote Sens.* **2021**, *13*, 1986. <https://doi.org/10.3390/rs13101986>

Academic Editor: Christophe Proisy

Received: 22 March 2021

Accepted: 16 May 2021

Published: 19 May 2021

Publisher's Note: MDPI stays neutral with regard to jurisdictional claims in published maps and institutional affiliations.



Copyright: © 2021 by the authors. Licensee MDPI, Basel, Switzerland. This article is an open access article distributed under the terms and conditions of the Creative Commons Attribution (CC BY) license (<https://creativecommons.org/licenses/by/4.0/>).

Keywords: China's mangrove forests; landscape pattern; spatial-temporal dynamic change analysis; remote sensing

1. Introduction

Mangrove is a unique woody plant community in the intertidal zone of tropical and subtropical coastal areas [1]. It is also one of the most productive ecosystems in the world [2]. Mangroves have ecological and socio-economic functions such as maintaining the water quality of coastal waters, blocking wind, fixing sand, maintaining biodiversity, and reducing coastal erosion [3]. However, the global area of mangroves decreased by 35% in the last two decades of the 20th century [4], and mangroves have become one of the most threatened ecosystems [5]. The carbon released into the atmosphere due to mangrove degradation accounted for 10% of the total emissions caused by deforestation [6]. Moreover, the level of fragmentation is still increasing, and patches of mangroves are gradually being split into smaller pieces [7]. The disappearance and fragmentation of mangroves are having

a significant impact on coastal populations and property in developing countries, especially in terms of destructive and life-threatening storms and floods [8,9]. Therefore, developing a scientific method of protecting and managing mangroves has attracted worldwide attention in recent years [10].

Since mangroves grow at the boundary between land and water, their habitats are mostly accompanied by muddy soil that is periodically submerged by tides [11]. Limited by accessibility, the use of traditional field investigation methods is often challenging when conducting large-scale mangrove research [12]. In recent years, remote sensing has been widely used in mangrove monitoring research due to its full coverage and multi-temporal advantages [13,14]. Monitoring studies have mainly included improvements to the classification accuracy of mangrove mapping using data and algorithms [15–19]; using remote sensing interpretation data to analyze the changes in the mangrove landscape pattern and analyzing the impact of mangrove degradation on the surrounding environment and economy [20,21]; and evaluating the adaptation of the mangrove habitat and the potential restoration area [5,22]. The main significance of these studies is that they provide better decision-making support for the conservation and management of mangroves. A fundamental requirement for mangrove conservation and restoration efforts is to obtain information about the current and historical mangrove distribution [23]. However, in the past 60 years, the focus of mangrove remote sensing research has evolved from mangrove distribution mapping and biophysical parameter inversion to ecosystem process characterization [12]. This change indicates that monitoring the distribution range of mangroves can no longer meet the current needs of mangrove protection and management, and further detailed information needs to be attained.

Mangroves have undergone rapid temporal and spatial changes worldwide, especially in developing regions [24]. As a developing country, China's mangrove area decreased by 44% from the 1950s to 2002 due to economic development and agricultural reclamation [25,26]. In recent years, the state and governments have strived to protect mangrove resources [27]. Through a series of measures, such as establishing protected zones and protection regulations and carrying out mangrove protection and restoration projects, the area of mangrove forests has gradually increased. Jia et al. [28] conducted an assessment of the conservation of mangrove forests in seven typical protected reserves based on area change. They pointed out that after 2000, the factors causing negative impacts on mangroves have gradually changed from human-made damage to natural disasters and artificial seawalls. However, due to the increased protection intensity, these two influences are not intuitively manifested by the area change. In addition, unscientific mangrove restoration methods may also lead to the loss of the ecological functions of mangroves. For example, mangrove restoration mostly relies on planting a single species, leading to the loss of animal and plant diversity [29]. In addition, planting mangroves in unsuitable habitats may result in low survival rates and increased fragmentation [30]. Studies have shown that the decrease in the total area of mangroves in China has been halted in recent years. However, the habitat status of mangroves outside nature reserves has not been significantly improved [31], and the community structure and ecological function of the mangroves in some areas have even shown signs of significant degradation [32]. Therefore, when assessing changes in mangrove forests and their impacts on the ecosystem, conclusions obtained solely by analyzing the area changes may be one-sided. It is necessary to assess the changes in the landscape pattern by analyzing the different landscape characteristics. However, there has been no study of the long-term dynamic changes in coastline mangroves throughout China, and most of the existing studies have focused on Guangdong or Hainan Province [33–36]. In addition, due to the small area of the mangroves in China, no specific spatial-temporal dynamic analysis of China's mangroves has been conducted on a global-scale. We know little about the landscape characteristics of China's mangroves on a national scale, except for the area changes. Therefore, there is a lack of nationwide and comprehensive landscape pattern research on mangroves in China.

The long-term analysis of mangrove landscape patterns would clarify the mangrove landscape pattern changes and the influence of natural factors and human activities on mangrove landscape patterns and dynamic processes [37,38]. Moreover, it would provide scientific support for mangrove conservation and restoration [12,39]. Therefore, such an analysis is crucial for assessing the effectiveness of national conservation efforts, understanding the responses of mangroves to climate change, and understanding the driving forces behind the changes in mangrove forests [28]. Furthermore, China's economy has grown rapidly in the past three decades, and most of the mangroves are distributed in the most densely populated areas. Thus, studies of China's mangroves can provide a good reference point for other developing countries with similar high-intensity human disturbances [40].

In this study, based on remote sensing interpretation data with a high classification accuracy for China's mangroves from 1978 to 2018 [41,42], the temporal and spatial changes in the landscape pattern of China's mangrove forests over the last 40 years were analyzed from multiple perspectives. By dividing the mangrove distribution area into 31 natural shores, we analyzed five landscape characteristics, i.e., the area, shape complexity, fragmentation, connectivity, and the integrated landscape state. The landscape spatiotemporal changes were analyzed by calculating the representative landscape index and clustering to provide scientific suggestions for mangrove protection management in China, and to provide a reference for mangrove protection in other areas of the world. A chart of the workflow of this study is shown in Figure 1. The main purposes of this study are (1) to analyze the spatial and temporal variations in the mangrove landscape pattern along China's coastline, and (2) to summarize the targeted protection opinions based on the changes from temporal and spatial viewpoints.

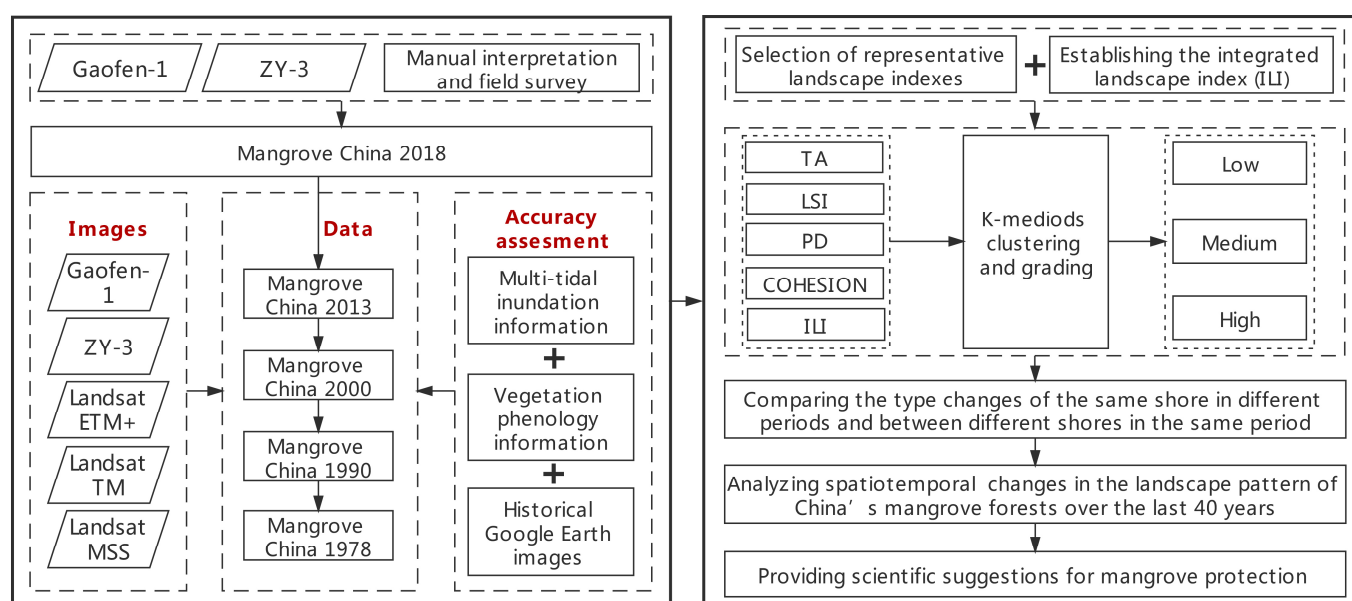


Figure 1. Workflow of this study.

2. Materials and Methods

2.1. Study Area

China's mangroves are mainly distributed in the intertidal zone in the coastal areas of southeastern China. The monitored area ranges from 18–29° N to 108–122° E (including 11,000 km of mainland coastline and about 3400 km of island coastlines). The northernmost city is Taizhou City, Zhejiang Province, and the southernmost city is Sanya City, Hainan Province. The surveillance area includes Hainan, the Guangxi Zhuang Autonomous Region (GZAR), Guangdong, Fujian, Zhejiang, Taiwan, Hong Kong, and the Macao Special Administrative Region. The geological conditions in the coastal area are complex. Estuaries

and bays are widespread, and the types of coastline are diverse, including silty coasts, sandy coasts, bedrock coasts, artificial coasts, and biological coasts. The topography, soil, climate, marine hydrology, and other conditions of the different regions in the study area are different. They determine the regional distribution differences of the mangroves to a certain extent. Therefore, before the temporal and spatial changes in China's mangrove landscape pattern were analyzed, it was necessary to determine the basic spatial units for analysis and evaluation. In this study, the coastal zone with mangroves in China were divided according to the following principles: (1) The entirety of an estuary or bay should be included within a shore to maintain their integrity, based on the natural geographical background of China's coastal zone. (2) The principle of shore length balance should be followed to keep the shore length moderate, and the difference between the shore lengths should not be too large in order to facilitate the comparison of different shores. (3) The spatial concentrated distribution areas of the mangroves should be included in the same shore as much as possible to reflect the growth and distribution of the mangroves. A long coastline without a mangrove distribution should be cut according to the length balance principle. (4) The entirety of a protected reserve should be included within a shore as much as possible in order to represent the protection of the mangroves.

Based on the above comprehensive division principles, a 20-km shoreline buffer zone was generated around the coastline. In the areas where mangroves are distributed along a river outside of the normal 20 km buffer zone, the buffer range was extended to include all of the mangrove distribution areas. Then, the study area was divided into 31 natural shores (Figure 2 and Table 1). Each shore was taken as a basic spatial unit, which helped to describe the zoning characteristics of the spatial distribution of the mangroves. Compared with using the entire study area or administrative division as a spatial unit, this method is more precise in terms of the spatial scale, so the results provide a strong foundation for regional mangrove protection and restoration strategies in China. For the details of the 31 natural shores, such as the information about terminal points and the administrative areas covered, please refer to reference [41].

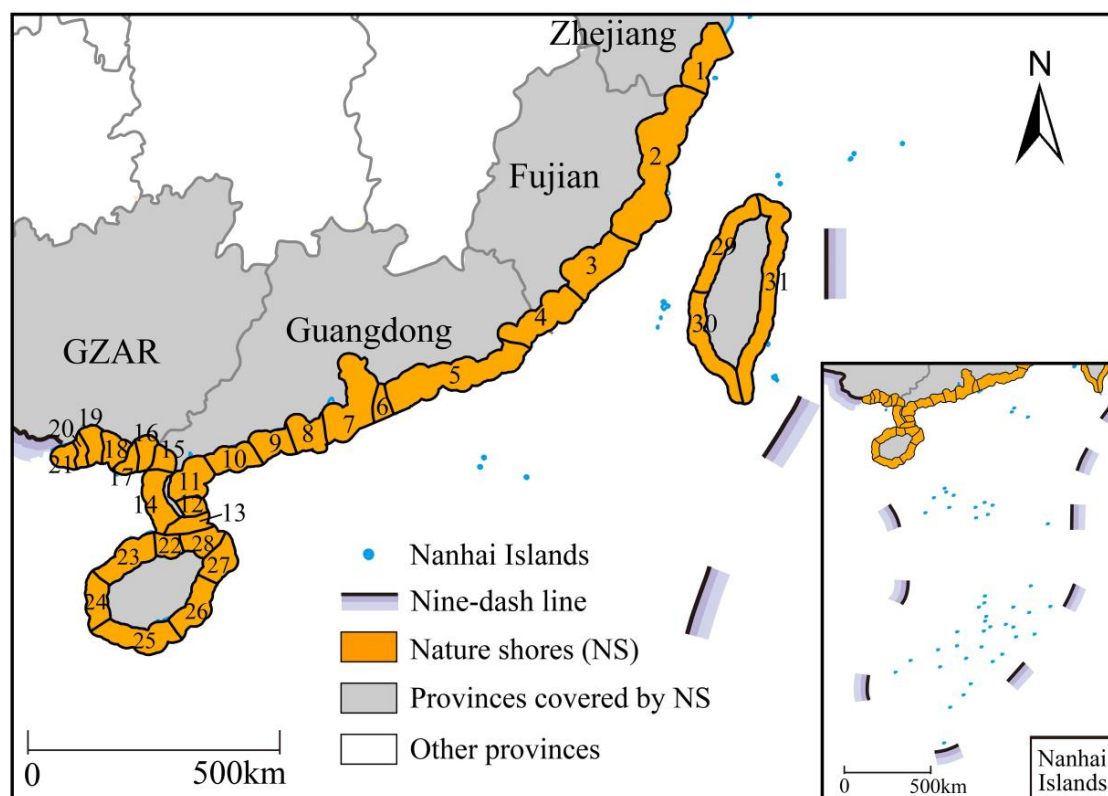


Figure 2. Distribution of the 31 natural shores.

Table 1. Basic information for China’s mangrove monitoring shores.

Province	Number	Name	
Zhejiang	1	Taizhou–Wenzhou Shore	
Fujian	2	Ningde–Fuzhou–Putian Shore	
	3	Quanzhou–Xiamen Shore	
	4	Yunxiao–Shantou Shore	
	5	Shantou–Hong Kong Shore	
Guangdong (for the convenience of statistics, the shores located in Hong Kong and the Macao Special Administrative Region were listed in Guangdong)	6	Shenzhen Bay Shore	
	7	The Pearl River Estuary Shore	
	8	Taishan–Enping Shore	
	9	Yangjiang Shore	
	10	Maoming Shore	
	11	Zhanjiang Port–Leizhou Bay Shore	
	12	Zhanjiang–Xinliao Shore	
	13	Zhanjiang–South Xuwen Shore	
	14	Zhanjiang–West Leizhou Shore	
	15	Zhanjiang–Anpu Shore	
	Guangxi Zhuang Autonomous Region (GZAR)	16	Shankou–Tieshan Port Shore
		17	Beihai Shore
		18	Hepu–Dafengjiangkou Shore
		19	Qinzhou Bay Shore
		20	Fangcheng Port Shore
21		Beilunhekou Shore	
Hainan	22	Haikou–Dongzhai Port Shore	
	23	Haiou–Lingaojiao Shore	
	24	Lingaojiao–Danzhou Shore	
	25	Dongfang Shore	
	26	Yinggehai–Sanya Shore	
	27	Wanning–Qionghai Shore	
	28	Hainan–Wenchang Shore	
Taiwan	29	Taipei–Taichung Shore	
	30	Tainan–Gaoxiong Shore	
	31	Taitung Shore	

2.2. Mangrove Distribution Data Based on Remote Sensing Interpretation

The research data mainly include five periods of mangrove distribution data for 1978, 1990, 2000, 2013, and 2018 (the canopy density of the mangrove patches is greater than 20%, and the area is greater than 100 m²). First, the mangrove distribution data for 2018 (MC 2018), which has an overall classification accuracy of 99.3%, was obtained based on the 2 m high-resolution images taken by the Gaofen-1 and ZY-3 Satellites through manual visual interpretation combined with field surveys [41,42]. The field surveys were conducted along the coastline of the Chinese mainland, from GZAR to Taizhou in Zhejiang. The length of the field survey route is approximately 9500 km. The classification accuracy of MC2018 was verified using 223 points obtained in the field survey and 2077 points obtained by the field investigator from high-resolution Google Earth imagery. Since our field route

did not include Taiwan, all of the verification points in Taiwan were from Google Earth. Compared with other existing mangrove distribution data, the resolution of the remote sensing images and the classification accuracy of the interpretation data, used in this study, have been greatly improved. By taking the MC2018 data as the basic data, the reverse time order and step-by-step interpretation strategies were adopted to interpret the mangrove distributions in 2013, 2000, 1990, and 1978. The images used for the historical periods are listed in Table 2.

Table 2. The images used in the historical data periods.

Year	Satellite	Sensor	Resolution
2013	Gaofen-1	PMS	2 m
	ZY-3	NAD and MUX	2 m
2000	Landsat7	ETM+	15 m
1990	Landsat5	TM	30 m
1978	Landsat1,2 and 3	MSS	60 m

Due to the fact that field survey data do not supplement the distribution of the mangroves in the historical periods, and the resolution of the remote sensing images taken in the historical periods is low (especially before 2000), the following three measures were taken to ensure the classification accuracy of the interpretation data used.

(1) Comprehensive interpretation of the mangroves was conducted based on multi-tidal inundation information: Most of the low mangroves on the tidal flat are submerged below the sea surface during high tide, so the remote sensing images taken at high tide contain less vegetation information than the real situation. If only the remote sensing images taken during high tide were used, the boundaries of the mangrove patches could not be accurately identified, and part of the low mangrove forest would be missed. Combining high tide and low tide images can ensure the classification accuracy of the interpretation data.

(2) The mangrove recognition was conducted based on vegetation phenology information: Large areas of cropland are distributed in China's coastal mudflats. During the growing season, the spectral characteristics of mangroves and crop vegetation are similar, so it is difficult to distinguish between them when using Landsat images (low resolution). The classification accuracy of the interpretation data can be guaranteed by combining multi-temporal images taken in the growing season and the crop harvesting season based on phenological information.

(3) Collaborative interpretation of the mangroves was conducted using Google Earth historical high-resolution images: Google Earth provides high-resolution images slices since 2000 in local areas. The level of the slices can reach 17 levels, and the resolution can reach about 1 m. Due to the low-resolution of the Landsat images, the Google Earth images were used to ensure the accuracy of the mangrove interpretation.

For the details of the interpretation process, please refer to references [41,42]. In addition, in the data for 1978, there was no mangrove distribution in NS1 (i.e., natural shore 1), NS25, and NS31. In the data for 1990 and 2000, there was no mangrove distribution in NS1 and NS31. Therefore, the total number of natural shores with mangrove distribution data for all five periods is 148 (28 + 29 + 29 + 31 + 31).

2.3. Selection and Calculation of the Landscape Index

Changes in mangrove cover have been shown to affect ecosystem services and ecological functions [43]. For example, patch shape and connectivity changes are closely related to patch stability, fish density, organic matter loss, and coastal protection [44–46]. The area attenuation and fragmentation of mangroves will lead to further multiple negative impacts such as reduced biodiversity and carbon storage capacity [22]. In addition, human activities (e.g., urban expansion) will lead to the simplification of patch shape, so the shape complexity can further reveal the influence of human activities on mangroves [47,48]. Therefore, when evaluating the temporal and spatial variations in the mangrove landscape pattern, it

is necessary to quantify more than the variation in the mangrove area. Landscape indexes can also be used to evaluate other landscape characteristics such as the shape complexity, patch fragmentation, and connectivity [49,50]. Some of the landscape indexes do not have practical ecological significance for this study, and some of the landscape indexes may represent different forms of the same ecological significance, that is, there is a high level of redundancy. Therefore, in this study, the landscape indexes were selected according to the following three principles; (1) whether the landscape index has a clear ecological significance; (2) whether the landscape index can reflect the landscape pattern characteristics within the study area; and (3) to ensure a low redundancy among the selected landscape indexes. According to the above principles, 1–2 representative landscape indexes were selected from each of the three types of landscape indexes (area and quantity type, shape type, and aggregation type) that are commonly used in current landscape index research, namely, the total area (TA), which represents the total area change; the patch density (PD), which represents the fragmentation; the landscape shape index (LSI), which represents the shape complexity; and COHESION, which represents the patch connectivity. The ecological meanings of and equations for these indexes are presented in Table 3, and the Spearman correlation coefficients [51] between them are given in Table 4. Since most landscape indexes are calculated using basic indicators, such as area, the number of patches, and edge lengths, the correlations between them are relatively high. Before calculating the landscape index, the shapefiles of the five periods of remote sensing interpretation were transformed into 10 km raster data, and then, the landscape indexes were calculated using the FRAGSTATS v4.2 software [52].

Table 3. The formulas for the representative indexes and their ecological significances.

Index	Formula	Units	Range	Ecological Significance
TA	$TA = A \left(\frac{1}{10000} \right)$ A: the total landscape area (m ²)	ha	TA > 0	TA was used to define the magnitude of the landscape. In landscape ecological construction, the area of the landscape is the most important factor used to maintain the stability of the ecosystem.
PD	$PD = \frac{N}{A} (10000) (100)$ N: Total number of patches in landscape	number (100 ha)	PD > 0	PD represents the patch fragmentation of the landscape. The higher the patch density, the greater the degree of landscape fragmentation. In addition, a higher patch density indicates that the landscape ecological process is active.
LSI	$LSI = \frac{0.25E^*}{\sqrt{A}}$ E*: The total length of the edge in the landscape	/	LSI ≥ 1	The shape complexity is measured by calculating the deviation between the patch shape and a circle or square with the same area. It can also indicate the intensity of human intervention. The larger the LSI, the more complex the shape, and the smaller the intensity of the manual intervention.
COHESION	$COHESION = \left[1 - \frac{\sum_{i=1}^m \sum_{j=1}^n P_{ij}^*}{\sum_{i=1}^m \sum_{j=1}^n P_{ij}^* \sqrt{a_{ij}^*}} \right] \cdot \left[1 - \frac{1}{\sqrt{Z}} \right]^{-1} \cdot (100)$ P _{ij} *: Perimeter of patch ij expressed as cell number; a _{ij} *: Area of patch ij expressed as cell number; Z: Total number of cells in the landscape	/	0 < COHESION < 100	COHESION can be used to measure the physical connectivity between patches and to characterize the habitat connectivity between patches. The higher the value, the better the connectivity between the patches.

Table 4. Spearman correlation coefficients among the representative landscape indexes.

	TA	LSI	PD	COHESION
TA	1.000	0.595 **	−0.550 **	0.389 **
LSI		1.000	0.191 *	−0.341 **
PD			1.000	−0.659 **
COHESION				1.000

** The correlation is significant at the 0.01 level (double tail); * The correlation is significant at the 0.05 level (double tail). Abbreviations: TA—total area, LSI—landscape shape index, PD—patch density.

2.4. Analysis of the Spatial and Temporal Changes in the Mangrove Landscape Pattern Based on the Landscape Indexes

In this study, the clustering method was used to analyze the temporal and spatial changes in the landscape patterns of the different shores. If the landscape pattern characteristics of a certain shore did not change significantly over the last 40 years, it was divided into the same type of shore after clustering. In contrast, if the data for the same shore in different periods could not be divided into the same type after clustering, the landscape pattern characteristics of the same shore were significantly different in the different periods, that is, the landscape pattern changed with time. In addition, for the same period, differences in the distributions of the types of landscape pattern characteristics in the different shores indicate that the changes in the landscape pattern are spatial. Based on the above analysis, the five periods of data were clustered. The temporal and spatial dynamic changes in the mangrove landscape pattern characteristics in China over the last 40 years were analyzed according to the corresponding types of changes in each shore in the different periods and the types of changes in the different shores in the same period.

The data used in this study has a small sample size, and the K-medoids clustering method has a better clustering performance for multi-feature data with a small sample size [53]. It is an improved algorithm based on K-means clustering. It is less affected by abnormal data or extreme data than the K-means method; that is, it is more robust than the K-means method when processing outlier data and noisy data. Therefore, the K-medoids algorithm was used to conduct the clustering in this study. In order to eliminate the dimensional influences of the different landscape indexes, the Z-score method was used to standardize the calculation results before clustering. The Z-score value was calculated by dividing the difference between the current value and the mean of the population by the standard deviation of the population [54]. Then, the K-medoids clustering method was used to cluster the normalized calculation results of each landscape index. The number of clusters was set to 3 by calculating the silhouette coefficient [55] (a measure of how similar an object is to its own cluster (cohesion) compared to other clusters (separation), details on selecting the optimal number of clusters are given in the Appendix A), and there were 148 samples in total, that is, the data for the same shore section in different periods were calculated as one sample. In the next step, the clustering results were sorted by numerical value. Taking COHESION as an example, 148 sample values were clustered into three categories and were sorted according to the COHESION value. The class with the smaller value was defined as low level and was assigned a value of 1; the class with the larger value was defined as high level and was assigned a value of 3; and the class with an intermediate value was defined as medium level and was assigned a value of 2. By comparing the type changes of the same shore in different periods and between different shores in the same period, the temporal and spatial changes in the connectivity of the mangroves in China were analyzed. The PD and LSI were also analyzed in this way. When the TA was analyzed, first the difference in the area changes in the different periods was calculated, and then, the difference value was clustered and classified.

2.5. Establishing and Analyzing the Integrated Landscape Index

Although the four representative landscape indexes selected above can reflect the spatial-temporal variations in the area change, fragmentation, connectivity, and shape

complexity, for the overall landscape, the changes in the landscape characteristics are not independent of each other, but rather they co-occur. In order to comprehensively describe the overall landscape pattern of the different shores under the spatial-temporal changes, in this study, an integrated landscape index (ILI) was constructed based on the calculation results and classification of the above four indexes. The ideal landscape pattern should have a high connectivity, a high shape complexity (low human disturbance), a low fragmentation, and no obvious reduction in total area. In order to expand the gap between the grades of each shore, the grading corresponding to the different landscape indexes was taken as the corresponding weight. As the impact of fragmentation on the state of the landscape pattern is negative, the weight is the grade value multiplied by -1. The ILI of the corresponding time can be obtained by multiplying and adding the weights and the landscape characteristic value of each shore. The specific equation is as follows:

$$ILI_{ij} = W_{C_{ij}} \times COHESION_{ij} + W_{L_{ij}} \times LSI_{ij} - W_{P_{ij}} \times PD_{ij} + R_{TA_{ij}} \quad (1)$$

where i is the shore number, $i = \{1, \dots, 31\}$; j is the time number, $j = \{1978, 1990, 2000, 2013, 2018\}$; $W_{C_{ij}}$ is the COHESION grade of the year j data for the i th shore; $COHESION_{ij}$ is the standardized calculation value of COHESION for the year j data for the i th shore; $W_{L_{ij}}$ is the LSI grade of the year j data for the i th shore; LSI_{ij} is the standardized calculation value of the LSI for the year j data for the i th shore; $W_{P_{ij}}$ is the PD grade of the year j data for the i th shore; PD_{ij} is the standardized calculation value of PD for the year j data for the i th shore; and $R_{TA_{ij}}$ is the difference between the standardized TA values for the i th shore in years j and $j - 1$, where the value of all of the bank sections in 1978 was set to 0.

After calculating the ILI values of all of the shores, the K-medoids method was used for the clustering and ranking. By comparing the types of changes for the same shore in different periods and between different shores in the same period, the temporal and spatial changes in the integrated landscape pattern of the mangroves in China were analyzed.

3. Results

3.1. Spatial and Temporal Variation Analysis of Four Landscape Characteristics

This section describes the dynamic changes of landscape pattern of Chinese mangroves in the past 40 years from the perspectives of time and spatial by analyzing the level changes of the same natural shores in different periods and the level changes of different natural shores in the same period in the clustering results. The detailed analysis will be carried out from the four aspects of total area, shape complexity, fragmentation, and connectivity.

3.1.1. Total Area

The temporal and spatial variations in the total area are shown in Figure 3 and Table 5. From 1978 to 1990, nearly half of the shores exhibited a decrease in area, mainly in the vast majority of the shores in Guangdong, southwestern Taiwan, and northern Hainan. In addition, the area of nearly one-third of the shores showed a slight increase, mainly in Zhejiang, Fujian, northern and eastern Taiwan, and southern Hainan. Only four shores showed a significant increase. During 1990–2000, the number of shores with reduced areas decreased, while the number of shores with increased areas increased significantly, mainly NS3 and NS4 at the junction of Fujian and Guangdong; NS6, NS7, and NS9 in the central part of Guangdong; and NS15 and NS16 at the junction of the Guangxi Zhuang Autonomous Region (GZAR) and Guangdong. It should be noted that the area changes of NS18 in GZAR and NS26 in southern Hainan changed from a slight increase to a decrease. During 2000–2013, the number of shores with reduced areas decreased further, with only five shores left, i.e., NS4 and NS5 in eastern Guangdong; NS11 and NS12 in southern Guangdong; and NS24 in northwestern Hainan. Nearly half of the shores showed a slight increase in area, mainly in Zhejiang, Northern Fujian, southern and northeastern Hainan, and eastern and southern Taiwan. However, the shores distributed in southern Fujian, western Guangdong, and GZAR showed a significant increase. The total area changes in 2013–2018 were consistent with the changes in the previous period. According

to the changes in the total area over the last 40 years, the areas in eastern Guangdong (NS4 and NS5), southwestern Guangdong (NS11 and NS12), and northwestern Hainan (NS24) have been decreasing, and the rest of the shores have been increasing at different levels. In general, the changes mainly occurred around 2000, which is reflected in the change in the direction of the area changes of some of the shores from decreasing to significantly increasing.

Table 5. Change in the level of the total area and the number of shores included.

Level	Mean Value of Total Area	Number of Shores Included in Each Period			
		1978–1990	1990–2000	2000–2013	2013–2018
Decrease (low)	−415.991	14	12	5	5
Slight increase (medium)	32.903	13	10	14	14
Significant increase (high)	299.058	4	9	12	12

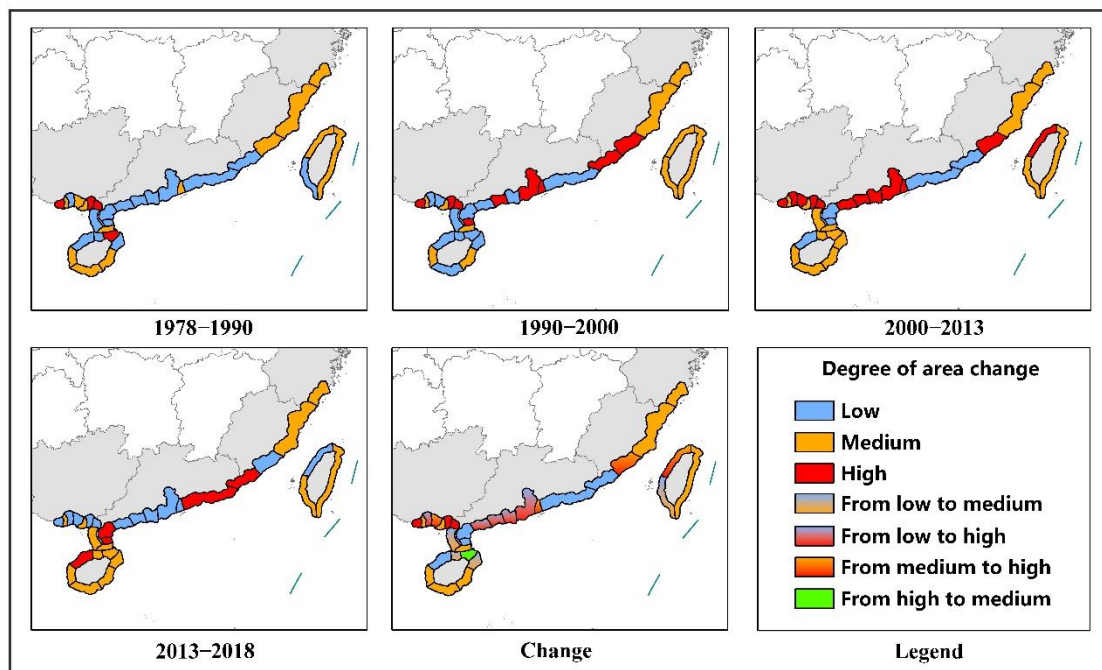


Figure 3. Temporal and spatial variations in the total area. In the legend, the low level indicates a decrease in area, the “Medium” level indicates a slight increase in area, and the high level indicates a significant increase in area.

3.1.2. Shape Complexity

The temporal and spatial variations in the shape complexity are shown in Figure 4 and Table 6. In 1978, the shapes of nearly two-thirds of the shores were relatively simple, except for most of the shores in Hainan and some in GZAR. From 1978 to 1990, the shape complexity of the shores in Fujian, eastern Guangdong, and Hainan did not change, while the shape complexity of the rest of the shores exhibited varying degrees of complexity changes. From 1990 to 2000, changes still occurred in western and southern Guangdong and northern Hainan, which was reflected by the change in the shape complexity of some of the shores from medium to high. From 2000 to 2013, the shape complexity changed significantly throughout the range, and the number of shores with simple shapes decreased rapidly. NS31 in eastern Taiwan, NS1 in Zhejiang, NS6 in central Guangdong, NS13 in southern Guangdong, and NS25 and NS27 in southern Hainan had simple shapes. The shape complexity level of most of the shores in western and southern Guangdong, GZAR, and northern Hainan changed to high. From 2013 to 2018, the shape complexity level of nearly two-thirds of the shores changed to high.

According to the trend of the changes over the last 40 years, the shapes of most of the shores have gradually become more complex, except for NS31 in eastern Taiwan, NS6 in central Guangdong, NS13 in southern Guangdong, and NS25 in southern Hainan. The main changes occurred from 2000 to 2013, which is reflected by the change in the shape complexity level from low to high. Since the shape complexity can further indicate the intensity of the influence of artificial disturbances on the mangrove landscape, through the above analysis, it was generally concluded that in 1978, the influence of artificial disturbances on the shores was generally strong. With time, the influence of the interference on the shores in southwestern Guangdong and northern Hainan initially gradually decreased, and then the influence on the other shores also began to decrease. However, NS6, NS15, and NS31 were always strongly affected by artificial interferences.

Table 6. Change in the level of the shape complexity and the number of shores included.

Level	Mean Value of LSI	Number of Shores Included in Each Period				
		1978	1990	2000	2013	2018
Low	7.595	18	16	13	6	4
Medium	14.238	7	10	9	8	7
High	23.699	3	4	7	17	20

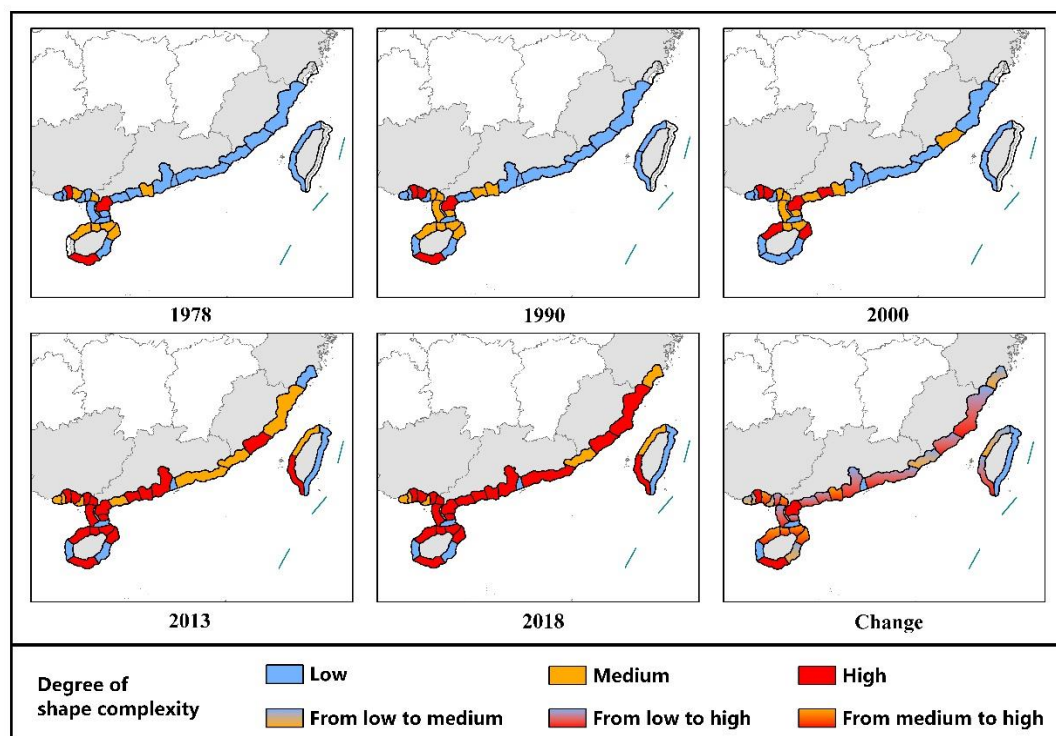


Figure 4. Temporal and spatial variations in the shape complexity.

3.1.3. Fragmentation

The temporal and spatial variations in the fragmentation are shown in Figure 5 and Table 7. In 1978, the overall fragmentation level was low, and only NS2 in Fujian, NS13 in southern Guangdong, and NS26 in southern Hainan were in states of high fragmentation. From 1978 to 1990, the fragmentation level remained relatively stable, and the overall fragmentation phenomenon did not worsen. NS30 in southwestern Taiwan, NS19 in GZAR, and NS23 in northern Hainan changed from low to medium, while the rest of the shores did not change. From 1990 to 2000, the fragmentation level changed slightly. In particular, the shores in eastern and southern Guangdong and some of the shores in GZAR changed

from low to medium. In general, the degree of fragmentation was not high. From 2000 to 2013, the fragmentation level changed significantly. NS6 in central Guangdong, NS15 and NS16 in western Guangdong, and NS28 in northeastern Hainan remained low. In contrast, the fragmentation levels of the rest of the shores deteriorated to varying degrees. Nearly two-thirds of the shores had medium levels of fragmentation, and only five shores located in Fujian, eastern Guangdong, and southern Hainan had high levels. From 2013 to 2018, the fragmentation level of NS31 in eastern Taiwan changed from medium to high, and there was no change in the rest of the shores.

According to the trend of the changes over the last 40 years, NS6 in central Guangdong, NS15 in western Guangdong, NS16 and NS21 in GZAR, and NS28 in eastern Hainan always maintained low levels of fragmentation; NS2 in Fujian, NS26 in southern Hainan, and NS13 in southern Guangdong always maintained high levels of fragmentation; and the fragmentation levels of the other shores increased to different degrees. The change from 2000 to 2013 was relatively large, and this change was mainly reflected by the change in the fragmentation level from low to medium.

Table 7. Change in the level of the fragmentation and the number of shores included.

Level	Mean Value of PD	Number of Shores Included in Each Period				
		1978	1990	2000	2013	2018
Low	8.914	24	22	17	5	5
Medium	28.838	1	4	9	21	20
High	103.1019	3	3	3	5	6

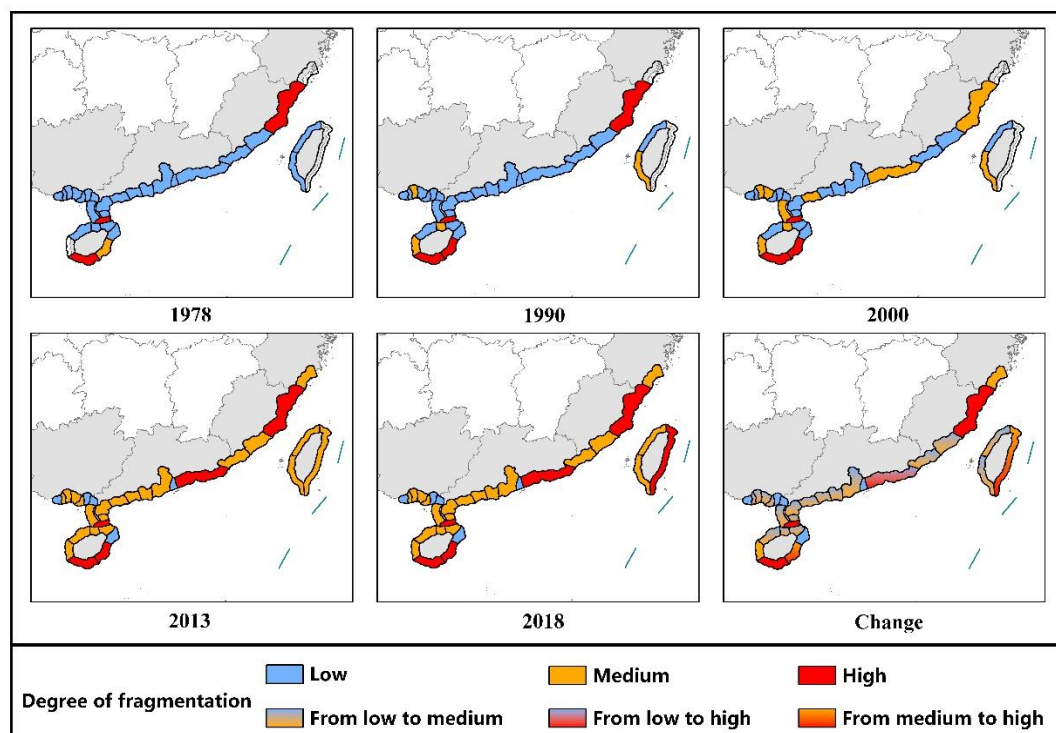


Figure 5. Temporal and spatial variations in the fragmentation.

3.1.4. Connectivity

The temporal and spatial changes in the connectivity are shown in Figure 6 and Table 8. In 1978, the connectivity level of the entire shoreline was high. Except for NS26 in southern Hainan, which was low, the connectivity levels of nearly two-thirds of the shores were high. From 1978 to 1990, the connectivity level fluctuated slightly. The main change

was that the levels of the shores located in Fujian and most of the shores in southwestern Guangdong changed from high to medium, and the level of NS27 in southeastern Hainan changed from medium to low. From 1990 to 2000, the connectivity situation deteriorated further, and nearly three-fourths of the shores had the medium levels. Only six shores in central Guangdong and northeastern Hainan remained at high levels. From 2000 to 2013, the connectivity deterioration mainly occurred in NS2 in northern Fujian; NS4, NS5, and NS13 in Guangdong; and NS20 and NS21 in western GZAR; while the connectivity of the rest of the shores did not change. From 2013 to 2018, except for the deterioration of NS1 and NS30, the connectivity of the rest of the shores did not change.

According to the trend in the changes in the connectivity over the last 40 years, NS22 and NS28 in northern Hainan and NS26 in southern Hainan remained at low levels; the shores in southern Fujian, southwestern Guangdong, and GZAR remained at medium levels or changed from high level to medium level; and the shores in northern Fujian, eastern Guangdong, and southeastern Hainan changed from high or medium-level to low level. The changes mainly occurred in 1978–2000, which shows that the connectivity levels of some of the shores changed from high to medium, and the deterioration was controlled after 2000.

Table 8. Change in the level of the connectivity and the number of included shores.

Level	Mean Value of COHESION	Number of Shores Included in Each Period				
		1978	1990	2000	2013	2018
Low	94.507	1	2	2	5	6
Medium	97.539	7	13	20	22	22
High	98.972	20	14	7	4	3

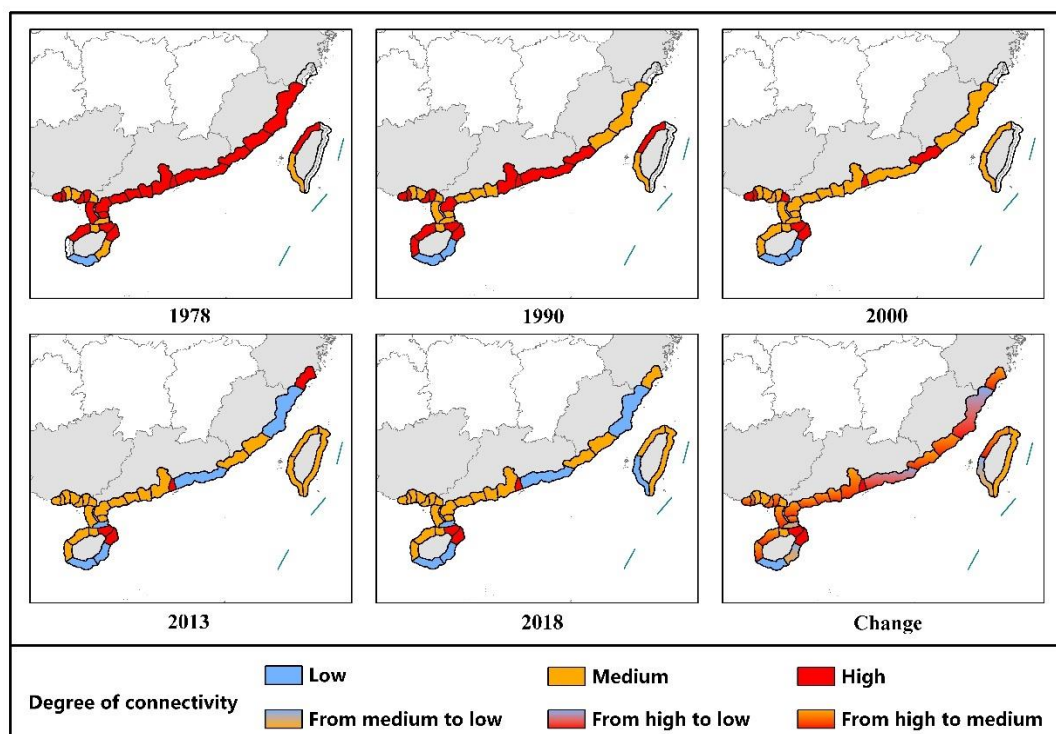


Figure 6. Temporal and spatial variations in the connectivity.

3.2. Spatial and Temporal Variation Analysis of the Integrated Landscape State

Through the analysis in Section 3.1, we have an understanding of the spatial and temporal changes of the four aspects of the landscape pattern of mangroves in China. In

this section, we will elaborate the spatial and temporal changes of the comprehensive landscape pattern by analyzing the clustering results of the ILI.

The temporal and spatial changes in the integrated landscape state are shown in Figure 7 and Table 9. In 1978, nearly half of the shores were high, mainly in Guangdong and northern Hainan; while the level of the shores in Fujian and western Taiwan was medium; and the level of NS26 and NS27 in southern Hainan and NS13 in southern Guangdong was low. From 1978 to 1990, the change was mainly reflected by the fact that the level of the shores in southwestern Guangdong decreased, changing from high to medium or from medium to low. In addition, the level of NS2 in Zhejiang also changed from medium to low. During 1990–2000, the change range was small, and the overall level continued to decline, except that the level of NS15 in southwestern Guangdong changed from medium to high. From 2000 to 2013, the levels of NS4 and NS5 at the junction of Fujian and Guangdong and NS20 and NS21 in GZAR still exhibited a downward trend. However, the levels of NS7 in central Guangdong, NS18 and NS19 in GZAR, and NS24 in northwestern Hainan changed from medium to high, and the overall integrated landscape states improved. During 2013–2018, the level of NS31 in eastern Taiwan changed from medium to low, and that of NS25 in southwestern Hainan changed from low to medium, while the levels of the other shores remained unchanged.

Table 9. Change in the level of the integrated landscape state and the number of shores included.

Level	Mean Value of ILI	Number of Shores Included in Each Period				
		1978	1990	2000	2013	2018
Low	−0.098	3	4	5	6	6
Medium	1.848	9	15	16	16	17
High	2.969	16	10	8	9	8

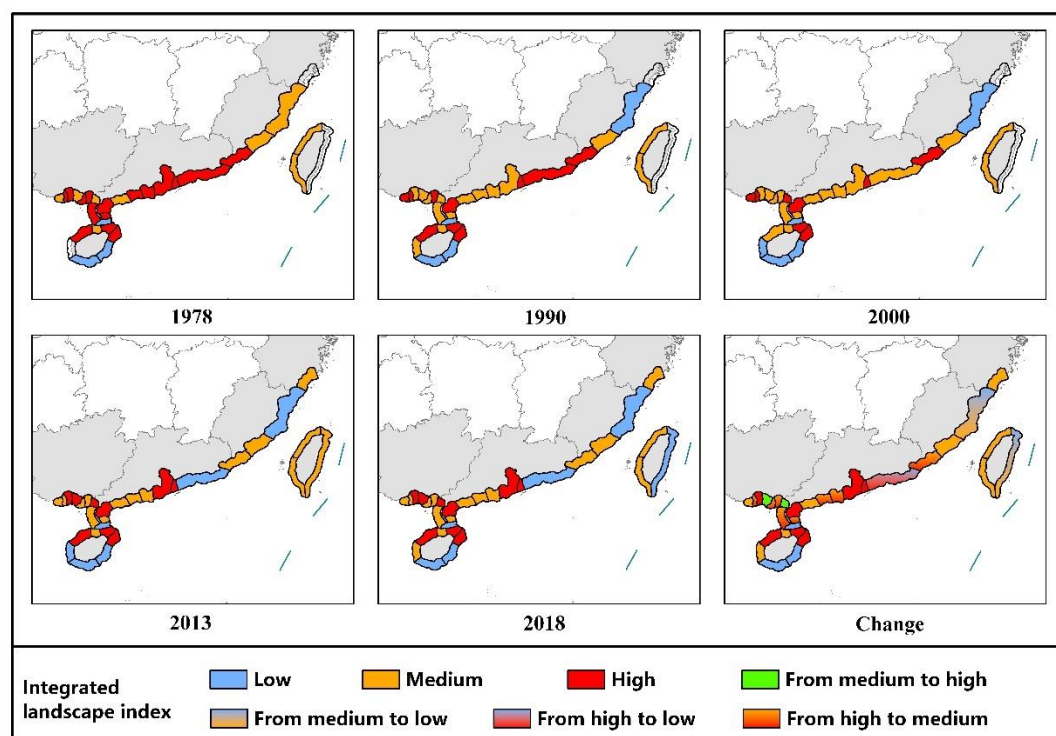


Figure 7. Temporal and spatial variations in the integrated landscape state.

According to the trend of the changes in the integrated landscape index over the last 40 years, NS26 and NS27 in southern Hainan Province always had low levels; NS1 in Zhejiang, NS3 in southern Fujian, NS9 in western Guangdong, and NS23 in Hainan always

had middle levels; and NS11 in southwestern Guangdong and NS22 and NS28 in eastern Hainan remained at high levels. In general, the integrated landscape states of nearly half of the shores exhibited a downward trend, but NS15 in western Guangdong and NS18 in eastern GZAR exhibited the opposite overall trend, that is, their levels changed from medium to high. The changes over the last 40 years were mainly reflected by the decrease in the levels from high to medium in some of the shores during 1978–1990.

4. Discussion

This study analyzed the temporal and spatial changes in China’s mangrove landscape pattern from five aspects: the total area change, shape complexity, connectivity, fragmentation, and integrated landscape state. In order to systematically illustrate the temporal and spatial changes in the landscape pattern of the mangroves in China over the last 40 years, the above analysis is summarized in Table 10. The corresponding changes in the mangrove patches when the levels of the different landscape characteristics change are shown in Figures 8 and 9. Figure 8 shows the changes in the mangrove patches under different TA levels. The TA level of NS10 was low during 1990–2000, and as can be seen from the figure, the mangrove patch area decreased significantly. The TA level was high during 2000–2013, and as can be seen from the figure, there was a significant increase in the mangrove patch area. The TA level of NS17 was medium during 1978–1990, with a slight increase in mangrove patch area. Figure 9 shows the mangrove patch changes as changes in the levels of the (a) shape complexity, (b) fragmentation, and (c) connectivity. The shape complexity levels of NS16 in 1978, 1990, and 2013 were low, medium, and high, respectively. As the level increased, the shape of the mangrove patches became increasingly complex. The degrees of fragmentation of NS20 were low and medium in 1990, and 2013, respectively, while that of NS13 was high in 1978. As the degree of fragmentation increased, as shown in the figure, the degree of fragmentation of the mangrove patches gradually increased. The connectivity level of NS13 was low in 2013, while those of NS12 were medium and high in 1990 and 1978, respectively. As the level increased, the connectivity of the mangrove patches gradually increased.

Table 10. Temporal and spatial variations in the mangrove landscape pattern in China over the last 40 years.

Landscape Characteristic	Spatial-Temporal Variation Characteristics		Individual Case (the Shore Numbers)	
	Temporal	Spatial	Always Low	Always High
Total area change	The area decreased from 1978 to 2000. After 2000, the area decreases gradually ceased and changed into increases.	The decrease in the area mainly occurred in Guangdong Province and northern Hainan Province.	4, 5, 11, 12, 24	15, 16, 21
Shape complexity	From 1978 to 2000, the shape complexity of most of the shores was relatively simple, that is, they were significantly affected by artificial interferences. After 2000, the shape complexity gradually increased, which means that the degree of artificial interference gradually weakened.	The initial change (increase) in the shape complexity was concentrated in southwestern Guangdong Province and northern Hainan Province, and then, it extended to most of the shores.	6, 13, 25, 27, 31	11, 19, 26
Fragmentation	From 1978 to 2000, most of the shores had a low degree of fragmentation. After 2000, the degree of fragmentation gradually increased.	Most of the shores exhibited continuous deterioration. The deterioration initially occurred in Fujian Province and northeastern and southwestern Guangdong Province, and then, it gradually extended to most of the shores.	2, 13, 26	6, 15, 16, 21, 28

Table 10. Cont.

Landscape Characteristic	Spatial-Temporal Variation Characteristics		Individual Case (the Shore Numbers)	
	Temporal	Spatial	Always Low	Always High
Connectivity	In 1978–2000, the overall connectivity continued to deteriorate. In 2000–2018, the deterioration of the connectivity was curbed, and some of the shores even improved.	The deterioration of the connectivity initially occurred in Fujian Province and southwestern Guangdong, and then, it extended to most of the shores. The shores in Fujian, northeastern Guangdong, and southern Hainan continued to deteriorate. The deterioration of the integrated landscape state initially occurred in southwestern Guangdong and the GZAR, and then, it gradually extended to most of the shores. The shores in Fujian, eastern Guangdong, and eastern Taiwan have been continuously deteriorating over the last 40 years.	26, 27	6, 22, 28
Integrated landscape state	In 1978–2000, the overall integrated landscape state continued to deteriorate. In 2000–2018, the deterioration of most of the shores was controlled.		13, 26, 27	6, 7, 11, 19, 24, 27, 28

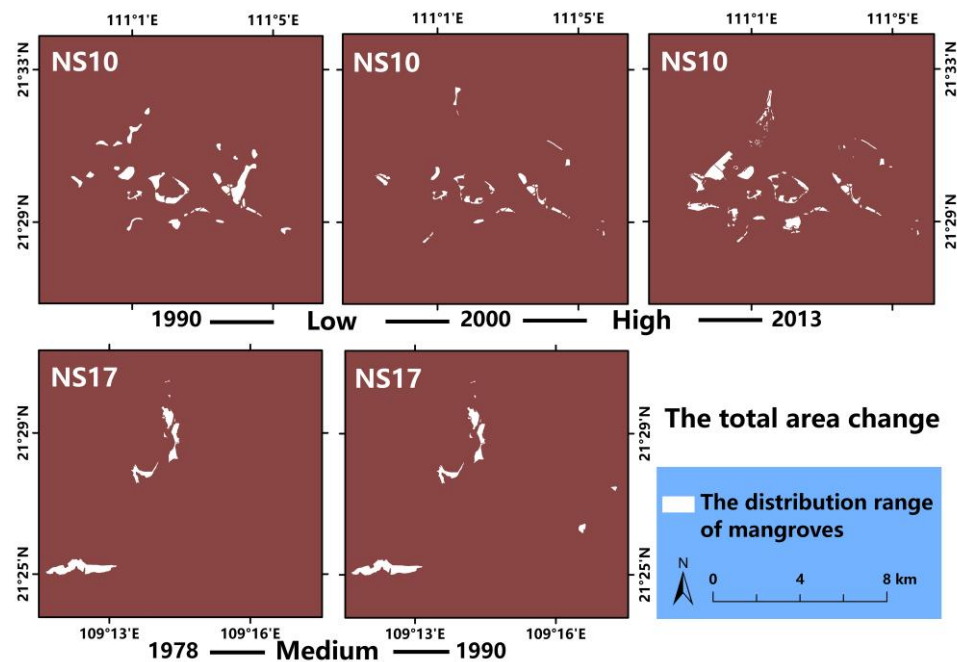


Figure 8. Mangrove patch changes for different levels of TA change.

The above analysis of the temporal and spatial changes in the different landscape characteristics shows that the same natural shore has different performances for the different landscape characteristics. For example, the poor connectivity of a certain shore does not mean that it has the same performance for the other landscape characteristics. Therefore, it is not sufficient or accurate to analyze one of the characteristics when comparing the landscape patterns of different shores. It is necessary to establish an integrated landscape index that can reflect the comprehensive state of the landscape. Taking the Zhanjiang–Anpu shore (NS15) as an example, the changes in the four landscape characteristics are as follows (Figure 10). The total area maintained a significant growth level over the last 40 years. The shape complexity was intermediate before 2000, and then, it became high, implying that the impact of artificial interferences decreased. The fragmentation remained at a low level, and the connectivity remained at a medium level over the last 40 years. There are obvious differences between the four different landscape characteristics. After calculating the ILI, it was found that the level of the integrated landscape state level was

medium before 2000, and then, it changed to high. Over the last 40 years, the integrated landscape state has gradually improved. According to some studies on mangrove in Zhanjiang [24,56,57], the largest mangrove protection area exists in the coastal area of mainland China, namely Zhanjiang mangrove protection area, distributed in NS15. The protection area was established in 1990 as provincial level and then upgraded to a national level in 1997. Prior to the year 2000, the mangrove habitat in Zhanjiang City was greatly threatened by human activities, mainly aquaculture. With the upgrading of the protection area and the implementation of a series of conservation regulations [58,59], the awareness of mangrove protection among local residents has gradually increased and the mangrove habitat has gradually improved. The results of landscape pattern analysis in this paper are basically consistent with the above rules. Moreover, since the Zhanjiang mangrove protection area was built in 1990 as provincial level, the integrated landscape pattern of mangroves in NS15 in the initial time (1978) was better than that in other natural shores without protection area or with city or county level protection area. This is also consistent with our analysis of the integrated landscape pattern state by calculating ILI. Therefore, the calculation of ILI obtains the information of the integrated landscape state, as well as facilitate the comparison of the landscape pattern state between different shores, which can be used to further guide regional mangrove protection and management in China.

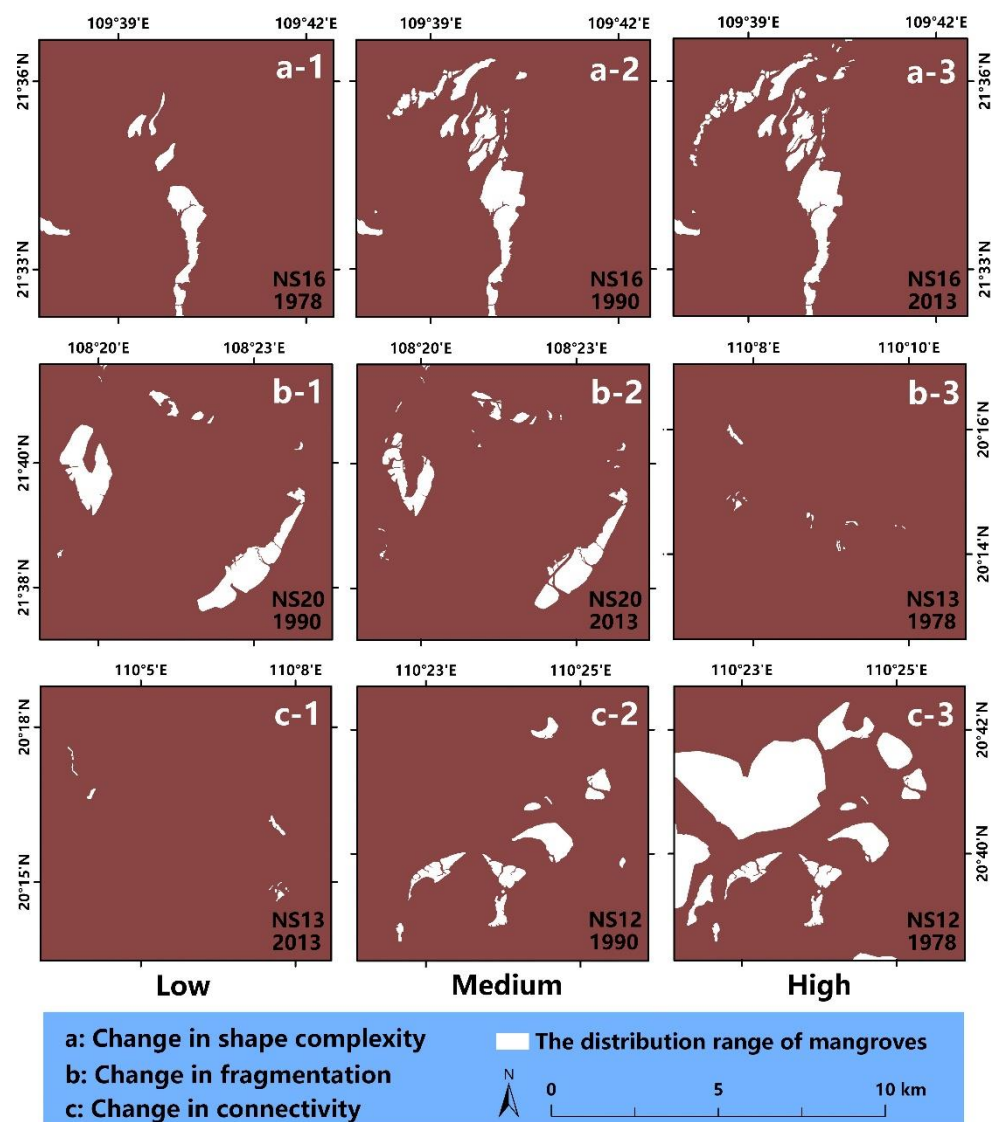


Figure 9. Mangrove patch changes for different levels of (a) shape complexity, (b) fragmentation and (c) connectivity.

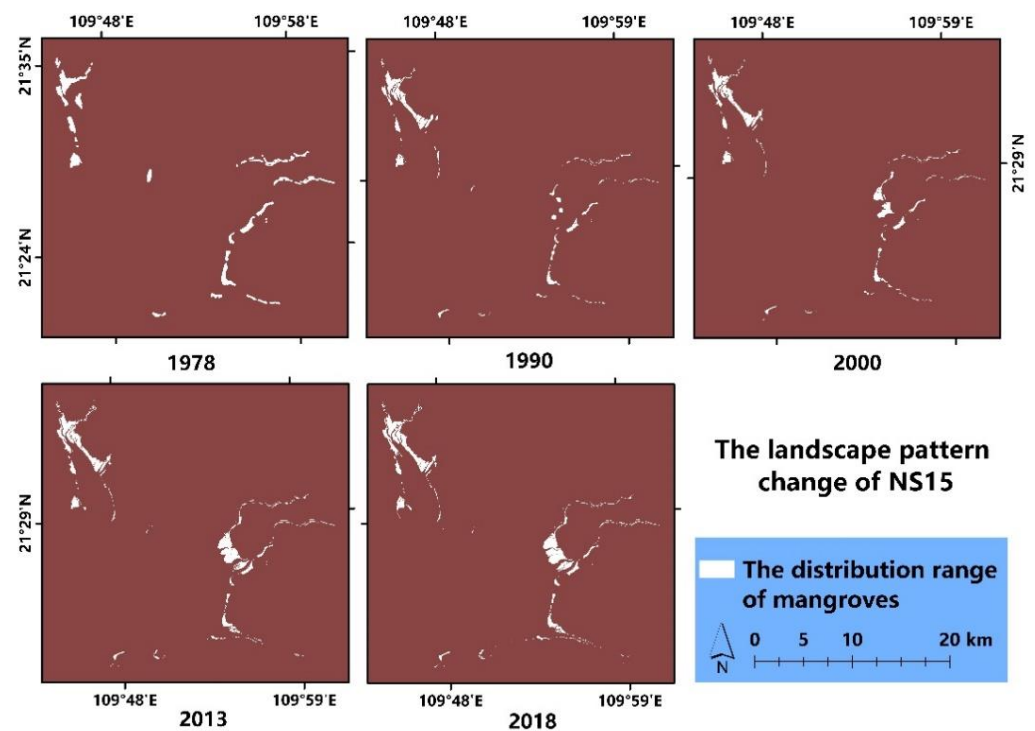


Figure 10. Landscape pattern changes of the Zhanjiang–Anpu shore (NS15) over the last 40 years.

Based on a comprehensive analysis of the temporal and spatial changes in the mangrove landscape pattern, this study provides scientific suggestions for protecting and managing mangroves in China from temporal and spatial viewpoints. From the temporal viewpoint, before 2000, the total area of the mangroves in China exhibited a downward trend, which was strongly affected by artificial disturbances. Moreover, the connectivity continued to deteriorate, while the degree of fragmentation remained stable at a low level. After 2000, the total area exhibited an upward trend, and the impact of human disturbances gradually weakened. In addition, the deterioration of the connectivity was controlled, but the degree of fragmentation gradually increased. The above phenomenon suggests that the effect of artificial disturbances on the connectivity of mangroves is relatively real-time, while their effect on fragmentation has a certain time lag. Since the reform and opening up, the mangrove habitat has been greatly damaged, and the area has been continuously reduced due to the economic drive of mariculture and urban development. After 2000, a series of protected areas and protection policies have been gradually established with increased reports and scientific research [40,60,61] on mangroves. Based on the current analysis results, it can be seen that the negative impact of development and aquaculture on the habitat before 2000 was demonstrated by the fragmentation characteristics after 2000. After 2000, due to increased conservation efforts, the area of the mangroves and the connectivity between patches were restored. However, the lag effect of fragmentation indicates that the mangrove fragmentation requires a certain period to improve after restoration measures are taken. Therefore, it is suggested that future mangrove protection and management should give priority to protection and should be supplemented by restoration. This proposal has also been confirmed in other mangrove studies [62–64]. For example, Schmitt et al. [65] recommended that the main mangrove management strategy should be to maintain the health of the remaining mangrove ecosystems (so as to improve their resilience) and to reduce the loss rate of mangroves, and conserving existing mangroves is usually more effective and cheaper than restoration.

From the spatial viewpoint, most of the shores located in Zhejiang, Fujian, GZAR, and Taiwan conform to the overall change trend. Moreover, there is little difference within the same province, and the overall change is consistent. However, the shores in Guangdong and Hainan are special. The landscape pattern of the Shantou–HongKong shore (NS5) in eastern Guangdong continued to deteriorate after 2000, while the landscape pattern of the Pearl River Estuary shore (NS7) in central Guangdong and the Zhanjiang–Anpu shore (NS15) in western Guangdong improved significantly. The landscape patterns of the Yinggehai–Sanya (NS26) and Wanning–Qinghai (NS27) shores in southern Hainan have been in a poor state (most of the time with low level) for the last 40 years, but the Haikou–Dongzhaigang (NS22), Lingaojiao–Danzhou (NS24), and Hainan–Wenchang (NS28) shores in northern Hainan have remained in a good state (most of the time with high level). Thus, there is an obvious difference in the landscape patterns in eastern and western Guangdong Province and southern and northern Hainan Province. According to the relevant reference [41], there are mangrove reserves above the provincial level on most of the shores with consistently good landscape patterns, such as NS22 and NS28. There are also national mangrove reserves on the shores where the landscape pattern has been significantly improved since 2000, such as NS15. In contrast, the shores with deteriorating landscape patterns and those that have exhibited consistently poor conditions not only experienced strong economic development, but their mangrove reserves were established later than in other areas. Most of these reserves are at the city or county level. Therefore, based on the above analysis, it is suggested that the mangrove habitat damage caused by economic development should be properly controlled along shores with poor landscape patterns, and the mangrove protection consciousness of the local government and residents should be improved. As was suggested in the above proposal, the protection of existing mangroves is more effective. However, artificial planting may need to be considered when the mangrove habitat is no longer self-correcting or self-renewing after loss or degradation even if the survival rate of mangrove afforestation is very low [40]. According to the State Forestry Administration [66], the survival rate of mangrove replantation in Guangdong Province in 2001 was less than 44%. Therefore, the traditional afforestation methods cannot be implemented in coastal areas. The foresters need to have a good understanding of mangrove ecology, coastal processes, and morphological dynamics (spatial and temporal), and they need to use them to make protection, planting, and management decisions [67]. The problems of the reduction of diversity and the outbreak of insects caused by planting a single species should also be considered. For more planting considerations, please refer to the following: (1) Ecological Mangrove Rehabilitation published by Lewis and Brown [68], which conducted a detailed assessment of the factors affecting mangrove establishment and early growth, and (2) the Global Mangrove Database and Information System (<http://www.giomis.com>) (accessed on 16 May 2021). This is a database of scientific literature, institutions, mangrove work, and regional projects and programs related to mangroves.

The methods and data accuracy of global mangrove remote sensing mapping are constantly improving. At present, there are many sets of global scale [17,23,69] and regional scale [70,71] mangrove distribution data based on medium or low-resolution images. Most of these data are used for small-scale mangrove area transfer analysis [72,73] or landscape pattern analysis [74,75]. These studies have helped to identify changes in mangroves, but the knowledge gained from remote sensing data seems to be similar. In terms of mangrove monitoring and protection, remote sensing data are accurate, fast, and cost-effective [76]. Therefore, developing a way to further explore the existing data in depth and to make full use of this resource should be further studied. Based on remote sensing data with a high classification accuracy, in this study, the landscape patterns of the mangroves in China over the past 40 years were analyzed from the perspectives of different landscape characteristics to encourage more research on mangroves and to mine the knowledge contained in remote sensing data.

5. Conclusions

In order to obtain the comprehensive information of landscape pattern change to provide scientific support for the protection and management of mangroves, this study analyzed the spatial and temporal changes of coastline mangrove landscape pattern in China over the last 40 years. This study was carried out from the perspective of the total area change, as well as from the perspective of shape complexity, connectivity, and fragmentation. In addition, the ILI (Integrated landscape Index) was constructed to evaluate the changes of the integrated landscape state and realize the rapid comparison between different shores. Based on the above analyses, we put forward two suggestions for protecting and managing mangroves from temporal and spatial.

(1) The management of mangroves should be focused on protection and supplemented by restoration. This study found that all the landscape features except the fragmentation were improved after 2000, which means that the change of fragmentation degree has a certain time lag. That is, the fragmentation requires a certain period to improve after restoration measures are taken. Therefore, the most effective way is to protect existing mangroves first.

(2) The mangrove habitat destruction caused by economic development should be properly controlled along shores with poor landscape patterns, and the mangrove protection consciousness of the local government and residents should be improved. This study found that the deterioration of the integrated landscape state initially occurred in southwestern Guangdong and the GZAR, and the shores in Fujian, eastern Guangdong, and eastern Taiwan have been continuously deteriorating over the last 40 years. Therefore, effective measures should be taken to protect the mangroves on the above shores. When there is a need for planting, it should be carried out after fully understanding the mangrove habitat and grasping the relevant precautions.

Author Contributions: Conceptualization, J.Z. and X.Y.; methodology, J.Z. and T.Z.; software, J.Z.; validation, J.Z., X.Y. and Z.W.; formal analysis, J.Z. and X.Y.; investigation, J.Z. and T.Z.; resources, T.Z. and X.Y.; data curation, J.Z. and X.L.; writing—original draft preparation, J.Z.; writing—review and editing, Z.W.; visualization, J.Z.; funding acquisition, X.Y. All authors have read and agreed to the published version of the manuscript.

Funding: This research was funded by the National Key Research and Development Program of China (Grant No. 2016YFC1402003); the National Science Foundation of China (Grant No. 41421001), and the Innovation Project of Laboratory of Resources and Environmental Information System (Grant No. O88RAA01YA).

Conflicts of Interest: The authors declare no conflict of interest.

Appendix A

In the clustering process, we calculated the silhouette coefficient [55] to determine the optimal number of clusters. The silhouette coefficient is a measure of how similar an object is to its own cluster (cohesion) compared to other clusters (separation). The rationality of the clustering results increases as the silhouette coefficient increases. We calculated the silhouette coefficient for 2–10 clusters, and the results are shown in Figure A1. As can be seen from the figure, the optimal number of clusters is 2–4. Due to the analysis of multiple landscape features, a unified number of clusters would facilitate the analysis and expression of the results and the calculation of the Integrated Landscape Index (ILI). We finally set the number of clusters to 3. The R code V4.0.3 used in the clustering process is shown presented in Figure A1.

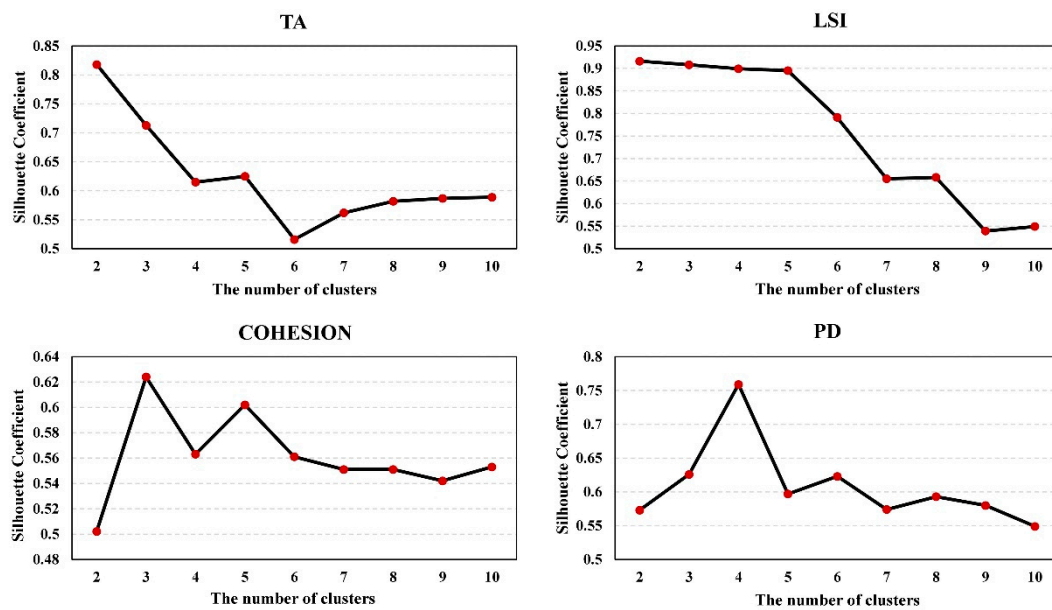


Figure A1. The variation in the silhouette coefficient with the number of clusters.

References

- Zhang, K.Q.; Thapa, B.; Ross, M.; Gann, D. Remote sensing of seasonal changes and disturbances in mangrove forest: A case study from South Florida. *Ecosphere* **2016**, *7*. [\[CrossRef\]](#)
- Alongi, D.M. Present state and future of the world's mangrove forests. *Environ. Conserv.* **2002**, *29*, 331–349. [\[CrossRef\]](#)
- Das, S.; Crepin, A.S. Mangroves can provide protection against wind damage during storms. *Estuar. Coast. Shelf Sci.* **2013**, *134*, 98–107. [\[CrossRef\]](#)
- Valiela, I.; Bowen, J.L.; York, J.K. Mangrove forests: One of the world's threatened major tropical environments: At least 35% of the area of mangrove forests has been lost in the past two decades, losses that exceed those for tropical rain forests and coral reefs, two other well-known threatened environments. *BioScience* **2001**, *51*, 807–815.
- Hu, W.J.; Wang, Y.Y.; Zhang, D.; Yu, W.W.; Chen, G.C.; Xie, T.; Liu, Z.H.; Ma, Z.Y.; Du, J.G.; Chao, B.X.; et al. Mapping the potential of mangrove forest restoration based on species distribution models: A case study in China. *Sci. Total Environ.* **2020**, *748*. [\[CrossRef\]](#) [\[PubMed\]](#)
- Donato, D.C.; Kauffman, J.B.; Murdiyarso, D.; Kurnianto, S.; Stidham, M.; Kanninen, M. Mangroves among the most carbon-rich forests in the tropics. *Nat. Geosci.* **2011**, *4*, 293–297. [\[CrossRef\]](#)
- Hu, L.J.; Xu, N.; Liang, J.; Li, Z.C.; Chen, L.Z.; Zhao, F. Advancing the mapping of mangrove forests at national-scale using Sentinel-1 and Sentinel-2 time-series data with google earth engine: A case study in China. *Remote Sens.* **2020**, *12*, 3120. [\[CrossRef\]](#)
- Barbier, E.B. The protective service of mangrove ecosystems: A review of valuation methods. *Mar. Pollut. Bull.* **2016**, *109*, 676–681. [\[CrossRef\]](#)
- Spalding, M.D.; Ruffo, S.; Lacambra, C.; Meliane, I.; Hale, L.Z.; Shepard, C.C.; Beck, M.W. The role of ecosystems in coastal protection: Adapting to climate change and coastal hazards. *Ocean Coast. Manag.* **2014**, *90*, 50–57. [\[CrossRef\]](#)
- Alongi, D.M. Mangrove forests: Resilience, protection from tsunamis, and responses to global climate change. *Estuar. Coast. Shelf Sci.* **2008**, *76*, 1–13. [\[CrossRef\]](#)
- Zhao, C.P.; Qin, C.Z. 10-m-resolution mangrove maps of China derived from multi-source and multi-temporal satellite observations. *ISPRS J. Photogramm.* **2020**, *169*, 389–405. [\[CrossRef\]](#)
- Wang, L.; Jia, M.M.; Yin, D.M.; Tian, J.Y. A review of remote sensing for mangrove forests: 1956–2018. *Remote Sens. Environ.* **2019**, *231*. [\[CrossRef\]](#)
- Green, E.P.; Clark, C.D.; Mumby, P.J.; Edwards, A.J.; Ellis, A.C. Remote sensing techniques for mangrove mapping. *Int. J. Remote Sens.* **1998**, *19*, 935–956. [\[CrossRef\]](#)
- Xia, J.S.; Yokoya, N.; Pham, T.D. Probabilistic mangrove species mapping with multiple-source remote-sensing datasets using label distribution learning in Xuan Thuy National Park, Vietnam. *Remote Sens.* **2020**, *12*, 3834. [\[CrossRef\]](#)
- Chen, B.Q.; Xiao, X.M.; Li, X.P.; Pan, L.H.; Doughty, R.; Ma, J.; Dong, J.W.; Qin, Y.W.; Zhao, B.; Wu, Z.X.; et al. A mangrove forest map of China in 2015: Analysis of time series Landsat 7/8 and Sentinel-1A imagery in Google Earth Engine cloud computing platform. *ISPRS J. Photogramm.* **2017**, *131*, 104–120. [\[CrossRef\]](#)
- Conchedda, G.; Durieux, L.; Mayaux, P. An object-based method for mapping and change analysis in mangrove ecosystems. *ISPRS J. Photogramm.* **2008**, *63*, 578–589. [\[CrossRef\]](#)
- Giri, C.; Ochieng, E.; Tieszen, L.L.; Zhu, Z.; Singh, A.; Loveland, T.; Masek, J.; Duke, N. Status and distribution of mangrove forests of the world using earth observation satellite data. *Glob. Ecol. Biogeogr.* **2011**, *20*, 154–159. [\[CrossRef\]](#)

18. Wang, D.Z.; Wan, B.; Qiu, P.H.; Su, Y.J.; Guo, Q.H.; Wang, R.; Sun, F.; Wu, X.C. Evaluating the performance of Sentinel-2, Landsat 8 and Pleiades-1 in mapping mangrove extent and species. *Remote Sens.* **2018**, *10*, 1468. [[CrossRef](#)]
19. Lymburner, L.; Bunting, P.; Lucas, R.; Scarth, P.; Alam, I.; Phillips, C.; Ticehurst, C.; Held, A. Mapping the multi-decadal mangrove dynamics of the Australian coastline. *Remote Sens. Environ.* **2020**, *238*. [[CrossRef](#)]
20. Seto, K.C.; Fragkias, M. Mangrove conversion and aquaculture development in Vietnam: A remote sensing-based approach for evaluating the Ramsar Convention on Wetlands. *Glob. Environ. Chang.* **2007**, *17*, 486–500. [[CrossRef](#)]
21. Herbeck, L.S.; Krumme, U.; Andersen, T.J.; Jennerjahn, T.C. Decadal trends in mangrove and pond aquaculture cover on Hainan (China) since 1966: Mangrove loss, fragmentation and associated biogeochemical changes. *Estuar. Coast. Shelf Sci.* **2020**, *233*. [[CrossRef](#)]
22. Bryan-Brown, D.N.; Connolly, R.; Richards, D.R.; Adame, F.; Friess, D.A.; Brown, C.J. Global trends in mangrove forest fragmentation. *Sci. Rep.* **2020**, *10*. [[CrossRef](#)] [[PubMed](#)]
23. Bunting, P.; Rosenqvist, A.; Lucas, R.; Rebelo, L.M.; Hilarides, L.; Thomas, N.; Hardy, A.; Itoh, T.; Shimada, M.; Finlayson, C.M. The global mangrove watch—A new 2010 global baseline of mangrove extent. *Remote Sens.* **2018**, *10*, 1669. [[CrossRef](#)]
24. Li, M.S.; Mao, L.J.; Shen, W.J.; Liu, S.Q.; Wei, A.S. Change and fragmentation trends of Zhanjiang mangrove forests in southern China using multi-temporal Landsat imagery (1977–2010). *Estuar. Coast. Shelf Sci.* **2013**, *130*, 111–120. [[CrossRef](#)]
25. Wang, W.; Wang, M. *China's Mangrove*; Science Press: Beijing, China, 2007.
26. Wu, P.; Zhang, J.; Ma, Y.; Li, X. Remote sensing monitoring and analysis of the changes of mangrove resources in China in the past 20 years. *Adv. Mar. Sci.* **2013**, *31*, 406–414.
27. Li, S.Z.; Xie, T.; Pennings, S.C.; Wang, Y.C.; Craft, C.; Hu, M.M. A comparison of coastal habitat restoration projects in China and the United States. *Sci. Rep.* **2019**, *9*. [[CrossRef](#)]
28. Jia, M.M.; Wang, Z.M.; Zhang, Y.Z.; Mao, D.H.; Wang, C. Monitoring loss and recovery of mangrove forests during 42 years: The achievements of mangrove conservation in China. *Int. J. Appl. Earth Obs.* **2018**, *73*, 535–545. [[CrossRef](#)]
29. Jia, M.M.; Wang, Z.M.; Zhang, Y.Z.; Ren, C.Y.; Song, K.S. Landsat-based estimation of mangrove forest loss and restoration in Guangxi Province, China, influenced by human and natural factors. *IEEE J. Stars* **2015**, *8*, 311–323. [[CrossRef](#)]
30. Zhang, X.H. Decision tree algorithm of automatically extracting mangrove forests information from Landsat 8 OLI imagery. *Remote Sens. Land. Res.* **2016**, *28*, 182–187.
31. Fan, H.; Wang, W. Some thematic issues for mangrove conservation in China. *J. Xiamen Univ. Natl. Sci.* **2017**, *56*, 323–330.
32. Ma, C.L.; Ai, B.; Zhao, J.; Xu, X.P.; Huang, W. Change detection of mangrove forests in coastal Guangdong during the past three decades based on remote sensing data. *Remote Sens.* **2019**, *11*, 921. [[CrossRef](#)]
33. Xin, K.; Huang, X.; Hu, J.L.; Li, C.; Yang, X.B.; Arndt, S.K. Land use change impacts on heavy metal sedimentation in mangrove wetlands—A case study in Dongzhai Harbor of Hainan, China. *Wetlands* **2014**, *34*, 1–8. [[CrossRef](#)]
34. Huang, X.; Xin, K.; Li, X.; Wang, X.; Ren, L.; Li, X.; Yan, Z. Landscape pattern change of Dongzhai Harbour mangrove, South China analyzed with a patch-based method and its driving forces. *Chin. J. Appl. Ecol.* **2015**, *26*, 1510–1518.
35. Yu, L.; Lin, S.; Jiao, X.; Shen, X.; Li, R. Ecological problems and protection countermeasures of mangrove wetland in Guangdong-Hong Kong-Macao Greater Bay Area. *Acta Sci. Nat. Univ. Pekin.* **2019**, *55*, 782–790.
36. Qiu, N.; Xu, S.; Qiu, P.; Yang, W.; Yang, Q. Community distribution and landscape pattern of the mangrove on the Qi'ao Island, Zhuhai. *Sci. Silvae Sinicae* **2019**, *55*, 1–10.
37. Li, T.; Zhao, Z.; Han, P. Detection and analysis of mangrove changes with multi-temporal remotely sensed imagery in the Shenzhen River Estuary. *J. Remote Sens.* **2002**, *6*, 364–369.
38. Fang, J. Analysis and Optimization of Green Space Landscape Pattern in Lankao County Based on GIS and FRAGSTATS. Ph.D. Thesis, Zhengzhou University, Zhengzhou, China, 2018.
39. Sasmito, S.D.; Taillardat, P.; Clendenning, J.N.; Cameron, C.; Friess, D.A.; Murdiyarso, D.; Hutley, L.B. Effect of land-use and land-cover change on mangrove blue carbon: A systematic review. *Glob. Chang. Biol.* **2019**, *25*, 4291–4302. [[CrossRef](#)]
40. Chen, L.Z.; Wang, W.Q.; Zhang, Y.H.; Lin, G.H. Recent progresses in mangrove conservation, restoration and research in China. *J. Plant Ecol.* **2009**, *2*, 45–54. [[CrossRef](#)]
41. Land Satellite Remote Sensing Application Center, Ministry of Natural Resources. *Remote Sensing Monitoring of Mangrove Resources in China (1978–2018)*; Geological Publishing House: Beijing, China, 2019.
42. Zhang, T.; Hu, S.; He, Y.; You, S.; Yang, X.; Gan, Y.; Liu, A. A fine-scale mangrove map of china derived from 2-meter resolution satellite observations and field data. *ISPRS Int. J. Geo. Inf.* **2021**, *10*, 92. [[CrossRef](#)]
43. Barau, A.S.; Qureshi, S. Using agent-based modelling and landscape metrics to assess landscape fragmentation in Iskandar Malaysia. *Ecol. Proc.* **2015**, *4*, 8. [[CrossRef](#)]
44. Drew, C.A.; Eggleston, D.B. Juvenile fish densities in Florida Keys mangroves correlate with landscape characteristics. *Mar. Ecol. Prog. Ser.* **2008**, *362*, 233–243. [[CrossRef](#)]
45. Sadro, S.; Nelson, C.E.; Melack, J.M. The Influence of landscape position and catchment characteristics on aquatic biogeochemistry in high-elevation lake-chains. *Ecosystems* **2012**, *15*, 363–386. [[CrossRef](#)]
46. Pace, M.; Borg, J.A.; Galdies, C.; Malhotra, A. Influence of wave climate on architecture and landscape characteristics of *Posidonia oceanica* meadows. *Mar. Ecol. Evol. Persp.* **2017**, *38*. [[CrossRef](#)]
47. Krummel, J.R.; Gardner, R.H.; Sugihara, G.; O'Neill, R.V.; Coleman, P.R. Landscape patterns in a disturbed environment. *Oikos* **1987**, *48*, 321–324. [[CrossRef](#)]

48. O'Neill, R.V.; Krummel, J.R.; Gardner, R.H.; Sugihara, G.; Jackson, B.; DeAngelis, D.L.; Milne, B.T.; Turner, M.G.; Zygmunt, B.; Christensen, S.W.; et al. Indices of landscape pattern. *Landsc. Ecol.* **1988**, *1*, 153–162. [[CrossRef](#)]
49. Manson, F.J.; Loneragan, N.R.; Phinn, S.R. Spatial and temporal variation in distribution of mangroves in Moreton Bay, subtropical Australia: A comparison of pattern metrics and change detection analyses based on aerial photographs. *Estuar. Coast. Shelf Sci.* **2003**, *57*, 653–666. [[CrossRef](#)]
50. Plexida, S.G.; Sfougaris, A.I.; Ispikoudis, I.P.; Papanastasis, V.P. Selecting landscape metrics as indicators of spatial heterogeneity—A comparison among Greek landscapes. *Int. J. Appl. Earth Obs.* **2014**, *26*, 26–35. [[CrossRef](#)]
51. De Winter, J.C.F.; Gosling, S.D.; Potter, J. Comparing the Pearson and Spearman correlation coefficients across distributions and sample sizes: A tutorial using simulations and empirical data. *Psychol. Methods* **2016**, *21*, 273–290. [[CrossRef](#)]
52. McGarigal, K. *FRAGSTATS Help*; University of Massachusetts: Amherst, MA, USA, 2015; p. 182.
53. Park, H.S.; Jun, C.H. A simple and fast algorithm for K-medoids clustering. *Expert Syst. Appl.* **2009**, *36*, 3336–3341. [[CrossRef](#)]
54. Mendenhall, W.M.; Sincich, T.L. *Statistics for Engineering and the Sciences*; CRC Press: Boca Raton, FL, USA, 2016.
55. Rousseeuw, P.J. Silhouettes: A graphical aid to the interpretation and validation of cluster analysis. *J. Comput. Appl. Math.* **1987**, *20*, 53–65. [[CrossRef](#)]
56. Leempoel, K.; Satyanarayana, B.; Bourgeois, C.; Zhang, J.; Chen, M.; Wang, J.; Bogaert, J.; Dahdouh-Guebas, F. Dynamics in mangroves assessed by high-resolution and multi-temporal satellite data: A case study in Zhanjiang Mangrove National Nature Reserve (ZMNNR), P.R. China. *Biogeosciences* **2013**, *10*, 5681–5689. [[CrossRef](#)]
57. Zhang, W.; Zhang, Y.; Zhang, H.; Chao, W.; Yang, L.; Jia, D.; Sun, R. Mangrove and the construction of regional ecological security pattern in Zhanjiang. *Geogr. Res.* **2010**, *29*, 607–616. [[CrossRef](#)]
58. Regulations of Guangdong Province on Wetland Protection. Available online: <http://www.zjhsl.org/html/quwugongkai/zhengcefagui/2013/1016/55.html> (accessed on 16 May 2021).
59. Regulations of the People's Republic of China on Nature Reserves. Available online: <http://www.zjhsl.org/html/quwugongkai/zhengcefagui/2013/1016/54.html> (accessed on 16 May 2021).
60. Peng, L. A review on the mangrove research in China. *J. Xiamen Univ. Nat. Sci.* **2001**, *2*, 592–603.
61. Zhang, Q.; Sui, S. The mangrove wetland resources and their conservation in China. *J. Nat. Resour.* **2001**, *16*, 28–36.
62. Samson, M.S.; Rollon, R.N. Growth performance of planted mangroves in the Philippines: Revisiting forest management strategies. *Ambio* **2008**, *37*, 234–240. [[CrossRef](#)]
63. Matsui, N.; Songsangjinda, P.; Morimune, K. Mangrove rehabilitation on highly eroded coastal shorelines at Samut Sakhon, Thailand. *Int. J. Ecol.* **2012**, *2012*, 1–11.
64. Duke, N.C. Mangrove reforestation in Panama: An evaluation of planting in areas deforested by a large oil spill. In *Restoration of Mangrove Ecosystems*; Field, C.D., Ed.; International Tropical Timber Organization, and International Society for Mangrove Ecosystems: Okinawa, Japan, 1996; pp. 209–232.
65. Schmitt, K.; Duke, N.C. *Mangrove Management, Assessment and Monitoring. Tropical Forestry Handbook*; Michael, K., Laslo, P., Eds.; Springer: Berlin/Heidelberg, Germany, 2015; pp. 1–29.
66. State Forestry Administration. Report of Mangroves Survey in China. 2002. Available online: <http://www.forestry.gov.cn/> (accessed on 16 May 2021).
67. Schmitt, K.; Albers, T.; Pham, T.T.; Dinh, S.C. Site-specific and integrated adaptation to climate change in the coastal mangrove zone of Soc Trang Province, Viet Nam. *J. Coast. Conserv.* **2013**, *17*, 545–558. [[CrossRef](#)]
68. Lewis, R.R.; Brown, B. Ecological Mangrove Rehabilitation—A Field Manual for Practitioners. Mangrove Action Project, Canadian International Development Agency and OXFAM. 2014. Available online: <https://blue-forests.org/wp-content/uploads/2020/04/Whole-EMR-Manual-English.pdf> (accessed on 16 May 2021).
69. Dahdouh-Guebas, F. World atlas of mangroves. *Hum. Ecol.* **2011**, *39*, 107–109. [[CrossRef](#)]
70. Souza, P.W.M.; Martins, E.D.; da Costa, F.R. Using mangroves as a geological indicator of coastal changes in the Braganca macrotidal flat, Brazilian Amazon: A remote sensing data approach. *Ocean Coast. Manag.* **2006**, *49*, 462–475. [[CrossRef](#)]
71. Long, J.B.; Giri, C. Mapping the Philippines' mangrove forests using Landsat imagery. *Sensors* **2011**, *11*, 2972–2981. [[CrossRef](#)]
72. Thomas, N.; Lucas, R.; Bunting, P.; Hardy, A.; Rosenqvist, A.; Simard, M. Distribution and drivers of global mangrove forest change, 1996–2010. *PLoS ONE* **2017**, *12*, e0179302. [[CrossRef](#)] [[PubMed](#)]
73. Phonphan, W.; Thanakunwutthirot, M. Mapping of mangrove change with remote sensing in Samut Songkhram Province, Thailand. In *International Conference on Human Interaction and Emerging Technologies*; Ahram, T., Taiar, R., Gremeaux-Bader, V., Aminian, K., Eds.; Springer: Cham, Switzerland, 2020; pp. 191–197.
74. Vaz, E. Managing urban coastal areas through landscape metrics: An assessment of Mumbai's mangrove system. *Ocean Coast. Manag.* **2014**, *98*, 27–37. [[CrossRef](#)]
75. Millan-Aguilar, O.; Nettel-Hernanz, A.; Hurtado-Oliva, M.A.; Dodd, R.S.; Flores-Cardenas, F.; Manzano-Sarabia, M. Landscape metrics and conservation status of five mangrove wetlands in the eastern gulf of California margin. *J. Coast. Res.* **2020**, *36*, 94–102. [[CrossRef](#)]
76. Seto, K.C.; Fragkias, M. Quantifying spatiotemporal patterns of urban land-use change in four cities of China with time series landscape metrics. *Landsc. Ecol.* **2005**, *20*, 871–888. [[CrossRef](#)]